Deformation and Unstable Flow in Hot Forging of Ti-6Al-2Sn-4Zr-2Mo-0.1Si

S. L. SEMIATIN AND G. D. LAHOTI

The stable and unstable plastic flow of Ti-6Al-2Sn-4Zr-2Mo-0.1Si (Ti-6242) has been investigated at temperatures from 816 to 1010 °C (1500 to 1850 °F) and at strain rates from 0.001 to 10 s^{-1} in order to establish its hot forging characteristics. In hot, isothermal compression, Ti-6242 with an equiaxed α structure deforms stably and has a flow stress which decreases with straining due to adiabatic heating. With a transformed-β microstructure, unstable flow in hot compression is observed and concluded to arise from large degrees of flow softening caused by microstructural modification during deformation and, to a small extent, by adiabatic heating. Both microstructures have a sharp dependence of flow stress on temperature. Using the concepts of thermally-activated processes, it was shown analytically that this dependence is related to the large strain-rate sensitivity of the flow stress exhibited by the alloy. From lateral sidepressing results, the large dependence of flow stress on temperature was surmised to be a major factor leading to the shear bands occurring in nonisothermal forging of the alloy. Shear bands were also observed in isothermal forging. A model was developed to define the effect of material properties such as flow softening rate and strain-rate sensitivity on shear band development and was applied successfully to predict the occurrence of shear bands in isothermal forging.

METALWORKING operations which involve large shape changes are normally done at elevated temperatures in excess of one-half of the homologous temperature of the workpiece material. At these temperatures, many metals tend to be very soft and ductile, and strains of the order of several hundred percent are not uncommon in bulk forming operations. Complex microscopic deformation processes are involved at these temperatures and strain levels. Hence, it has been only in the last fifteen or so years that an understanding of what actually occurs during hot working has been sought to any degree.[1]

At hot working temperatures, dynamic softening processes compensate for strain hardening, and the flow stress (as measured in a simple tension or uniform compression test) does not necessarily increase with straining. In single-phase metals, the dynamic softening processes are typically either dynamic recovery or dynamic recrystallization.[2,3] Metals with relatively high stacking fault energies at hot working temperatures (*e.g.*, α-iron, commercial purity aluminum) dynamically recover. Metals with low stacking fault energies (*e.g.*, γ-iron, copper) usually soften during hot working primarily by a process of dynamic recrystallization. Softening at elevated temperatures may occur by mechanisms other than dynamic recovery and dynamic recrystallization and should be considered when interpreting high temperature flow stress data.[4] These mechanisms include adiabatic heating,[5] spherodization of lamellar two-phase structures, precipitate coarsening, and development of soft textures.

An understanding of the various deformation and softening mechanisms in hot working is helpful in developing sound processing sequences and avoiding defects in finished parts. These defects include brittle failures due to hot shortness,[6] grain boundary and triple point cracks,[7] and void generation (cavitation).[8] Another possible defect, in hot forging in particular, is that of shear bands, or regions of localized deformation crossing many grains.[9] During deformation processing, these regions of intense deformation and heat develop at the interface between adjacent areas of discontinuous deformation such as that between regions of deforming and nondeforming (*i.e.*, dead) metal.[10] Because the width of the interface can be infinitesmal, even small bulk strains can produce shear strains of the order of several thousand percent. Once initiated, a shear band may become self-propagating because the essentially adiabatic heating at the interface produces a marked drop of the local flow stress. As a result, localized phase changes or fracture may occur.

Depending on the alloy, various combinations of process variables (tool and workpiece geometry, deformation rate, preheat temperature, die temperature, lubrication) and material parameters (strain-rate sensitivity of the flow stress, temperature dependence of the flow stress, strain-hardening rate, thermal conductivity, specific heat, phase transformation kinetics) have been observed to lead to the development of shear bands. This problem has been observed in both cold and hot forging of alloys such as aluminum alloys,[11-13] carbon and alloy steels,[14-17] titanium alloys,[18-20] and nickel-base alloys.[20] Forged parts of these materials are found frequently in service applications requiring high performance. Hence, it is critical that the development of shear bands during metalworking and their possible effects on service properties be understood.

Two-phase (α/β) titanium alloys are particularly susceptible to shear bands during hot forging.[20] The sharp dependence of flow stress on temperature, low strain-hardening rate, and poor thermal conductivity

S. L. SEMIATIN is Principal Research Scientist and G. D. LAHOTI is Senior Research Scientist, Metalworking Section, Battelle's Columbus Laboratories, Columbus, OH 43201.

Manuscript submitted July 14, 1980.

ISSN 0360-2133/81/1012-1705$00.75/0

characteristic of these alloys[21-24] contribute to the occurrence of shear bands. The investigation reported here was undertaken to establish the occurrence of shear bands in a typical α/β titanium alloy—Ti-6Al-2Sn-4Zr-2Mo-0.1Si (Ti-6242), an alloy which is receiving increasing attention in jet-engine applications.[25] To characterize the deformation behavior of the alloy, isothermal, hot-compression tests were conducted over a range of temperatures and strain rates. The deformation mechanisms involved were inferred from the flow stress curves and metallography. These results were employed in the interpretation of observations of shear bands developed in both nonisothermally-sidepressed cylinders as well as isothermally-sidepressed cylinders.

EXPERIMENTAL PROCEDURES

Material

The material used was Ti-6242. Initially, the billets had been melted and broken down by RMI Company of Niles, Ohio and had been analyzed to have a β transus temperature of 988 °C (1810 °F) and chemistry (in wt pct) of 6.0 aluminum, 2.2 tin, 4.1 zirconium, 2.0 molybdenun, 0.09 silicon, balance titanium. The billets were then forged by Wyman-Gordon Company of North Grafton, Massachusetts and supplied in the form of 15.88 cm (6.25 in.) diam billets. Forging was accomplished at 954 °C (1750 °F) after which the billets were heat treated at 968 °C (1775 °F) for 2 h and air cooled. As received, the microstructure consisted of equiaxed α (α grain size = 11 μ) in a transformed β matrix, hereafter referred to as the $\alpha + \beta$ microstructure.[25] Some of the material was heat treated at 1010 °C (1850 °F) for 30 min and air cooled to produce an acicular, transformed β microstructure, hereafter referred to as the β microstructure.[25] The prior β grain size of this structure was 350 μ.

Isothermal Compression Testing

Isothermal compression testing was used to characterize the stress-strain behavior of the titanium alloy and to study its flow phenomenology at hot working temperatures. Compression specimens measuring 1.27 cm (0.50 in.) diam × 1.91 cm (0.75 in.) high were machined from bar stock of material having both the $\alpha + \beta$ as well as β microstructures. They were cut in either the axial (longitudinal) direction or the transverse direction. In addition, specimen ends had shallow grooves for lubricant retention at hot working temperatures. After thorough cleaning of the specimens, glass coatings, which provided lubrication and protection from the atmosphere at test temperatures, were applied. The coatings used were Deltaglaze 93 (816, 871, 913 °C [1500, 1600, 1675 °F]), Deltaglaze 347M (954 °C [1750 °F]), and Deltaglaze 69 (1010 °C [1850 °F]), all made by Acheson Colloids Company of Port Huron, Michigan.

A test fixture with superalloy tooling (Fig. 1) was constructed to run the hot isothermal compression tests on a closed-loop electrohydraulic-testing machine. The tooling design is based on one originally employed by Kuhn.[26] Using a 5 kW Applied Test Systems resistance furnace, the test fixture was heated to test temperatures in 1 h. Furthermore, the fixture is sufficiently massive to provide temperature equilibration within 3 min after furnace opening to enable insertion of test specimens. Prior to testing, specimens were heated *in situ* on the hot compression tooling for a total of 13 to 15 min. Of this preheat time, approximately 3 min were required for the specimen to attain test temperature.

Specimens of both microstructures ($\alpha + \beta$ and β) were compressed to 50 pct reduction in height at constant true strain rates of 0.001, 0.1, 1.0, and 10.0 s^{-1}. An RC electrical circuit provided the required exponential signal to control the ram of the testing machine to obtain the constant strain rate. The $\alpha + \beta$ microstructure was tested at temperatures T = 816, 871, 913,

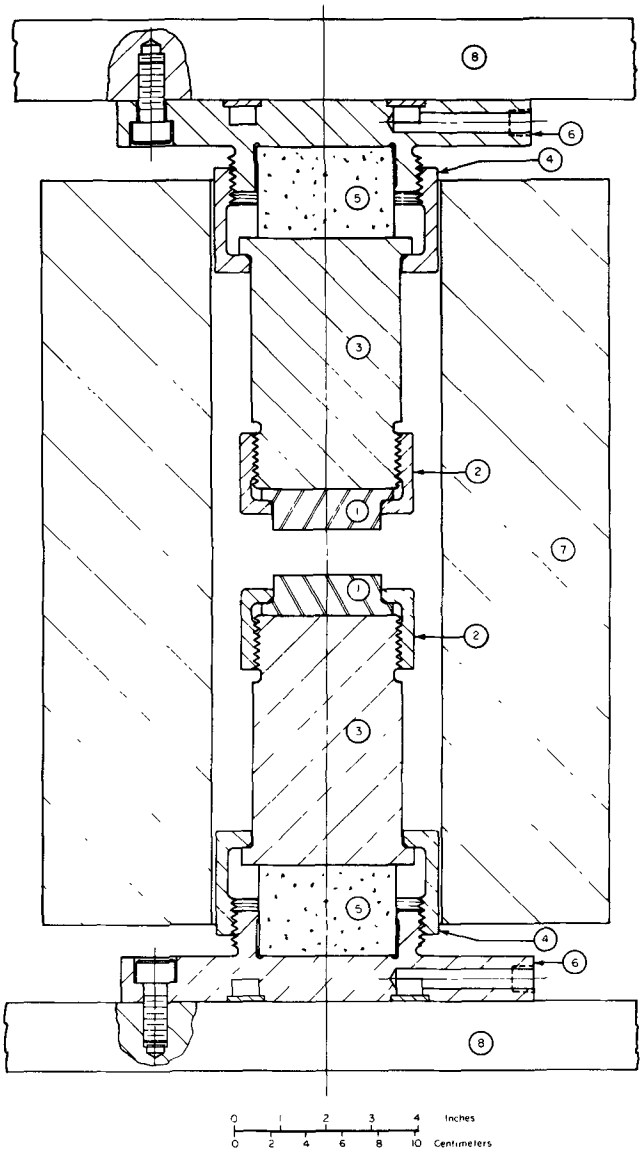

Fig. 1—Hot-isothermal compression test fixture. (1 = superalloy compression die, 2 = superalloy die retainer ring, 3 = superalloy die support, 4 = stainless steel support retainer ring, 5 = ceramic insulator, 6 = stainless steel compression tooling base with channel for water cooling, 7 = resistance furnace, 8 = two-post die set.)

954, and 1010 °C (1500, 1600, 1675, 1750, and 1850 °F). The β microstructure was characterized only at the first four of these temperatures since at 1010 °C (1850 °F), both microstructures revert to the single-phase bcc microstructure.

Load-time and stroke-time* data were obtained using a high speed recorder (Gould Inc., Model No. 2007-4290-00), digitized using a Summagraphics digitizer (Model ID-1-CTR-17), and finally reduced to load-stroke data or stress-strain data using the following expressions:

* Stroke-time data were checked to verify that the true strain-rate, $\dot{\epsilon}$, varied no more than 3 pct during any one compression test.

$$\epsilon = \dot{\epsilon} t,$$

and

$$\sigma = \frac{F}{A_o} \exp \epsilon.$$

$\epsilon, \dot{\epsilon}$ = true axial strain, strain rate; t = time; σ = true axial stress; F = applied load; A_o = initial specimen cross-sectional area. From measurements of friction factors, it was determined that the stress-strain data so determined were in error by no more than 4 pct, and, thus, corrections for friction were not applied. These data were used in conjunction with metallography on deformed specimens to establish the phenomenology of plastic flow for the two microstructures at the various test temperatures and strain rates. In addition, they were used to determine the strain rate sensitivity parameter, m:

$$m = \left. \frac{\partial \ln \sigma}{\partial \ln \dot{\epsilon}} \right|_{\epsilon,T}. \qquad [1]$$

Nonisothermal Sidepressing

Nonisothermal lateral sidepressing (*i.e.*, diameterical compression) of cylindircal specimens was chosen to simulate a typical hot-forging process for titanium alloys—the conventional forging of jet engine compressor blades—and to determine the susceptibility of Ti-6242 and similar alloys with strong flow stress dependence on temperature to shear bands brought about by die chilling. Longitudinal specimens of both microstructures were forged. They measured 1.02 cm (0.400 in.) diam × 10.16 cm (4.00 in.) long. Coated with Deltaglaze 93, the specimens were preheated for 15 min at 913 °C (1675 °F) and then forged between flat tool steel dies heated to 204 °C (400 °F). Reductions to final thicknesses of either 0.51 or 0.25 cm (0.20 or 0.10 in.) were imposed in order to establish how shear bands develop with straining. In all cases, shear bands were detected through metallographic means.

The sidepressing operations were performed in a 4.45 × 10^6 N (10^6 lb) Erie mechanical press of scotch-yoke design.[27] In presses such as this, the ram velocity varies sinusoidly from a maximum value at the top of the stroke to zero at the bottom of the stroke (*i.e.*, at the bottom dead center). The ram velocity at impact in these experiments was of the order of 36 cm/s (14 in./s), and, hence strain rates were of the order 35 s^{-1}. By slowing the press flywheel, the strain rates during sidepressing can be varied. Tests at other strain rates as well as tests with different specimen preheat temperatures in the range 816 to 1010 °C (1500 to 1850 °F) and die temperatures are being run. Results from these tests are similar, and a more in-depth summary of nonisothermal sidpressing will be published in the future.

Isothermal Sidepressing

Isothermal lateral sidepressing of cylindrical specimens of Ti-6242 was performed to eliminate the effects of die chilling on shear band development and to establish the material variables which control shear band development in isothermal forging situations. Longitudinal specimens of both microstructures, measuring either 0.71 cm (0.280 in.) diam × 2.54 cm (1.00 in.) long or 1.27 cm (0.50 in.) diam × 1.91 cm (0.75 in.) long, were preheated (for 15 min) and forged in a can-like superalloy jig with titanium carbide anvils.[28] Coated with Deltaglaze 93, these specimens were tested at 843 and 913 °C (1550 and 1675 °F) in the Erie mechanical press. They were forged to a final thickness of 0.23 cm (0.090 in.). For these trials, the press flywheel was slowed to give a ram impact velocity of 13.7 cm/s (5.40 in./s), and, hence, strain rates were of the order of 10 s^{-1}. Shear bands were detected using metallographic sections.

RESULTS AND DISCUSSION

Isothermal Compression Testing

Compresssion Load-Stroke Curves. Sample load-stroke curves at 0.1 and 1.0 s^{-1} are shown in Fig. 2. Curves for the other two strain rates are similar. Although there was little difference in data from specimens cut longitudinally *vs* those cut transversely for a given microstructure, there is a marked difference between the basic behavior of $\alpha + \beta$ and β material. The load-stroke curves for the $\alpha + \beta$ microstructure increase monotonically, whereas the β load-stroke curves are generally decreasing or constant with respect to stroke. From these data, one might expect uniform flow for the $\alpha + \beta$ specimens and nonuniform flow arising from load instability for the β specimens.[4,29,30] For the $\alpha + \beta$ specimens, flow was indeed uniform with only slight bulging arising from frictional effects. For the β specimens, there was slightly more nonuniform flow than for the $\alpha + \beta$ specimens. In addition, the specimen surfaces were rumpled, an effect which can be attributed to the large prior β grain size of this structure. These results contrast to the grossly nonuniform flow of β specimens upset in a mechanical press,[31] but are similar to results reported by Dadras and Thomas for similar constant strain rate tests.[32] In the mechanical-press-compression tests,[31] however, the decrease of strain rate with increasing stroke led to somewhat larger load drops, which would have been more effective in triggering the unstable flow. Misalignment of the compression jig in the mechanical press tests could also have been a more effective triggering device.

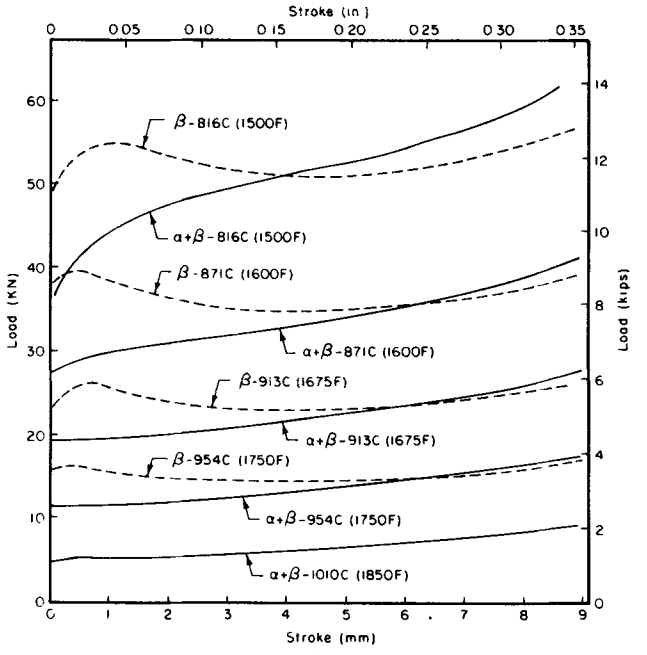

(a)

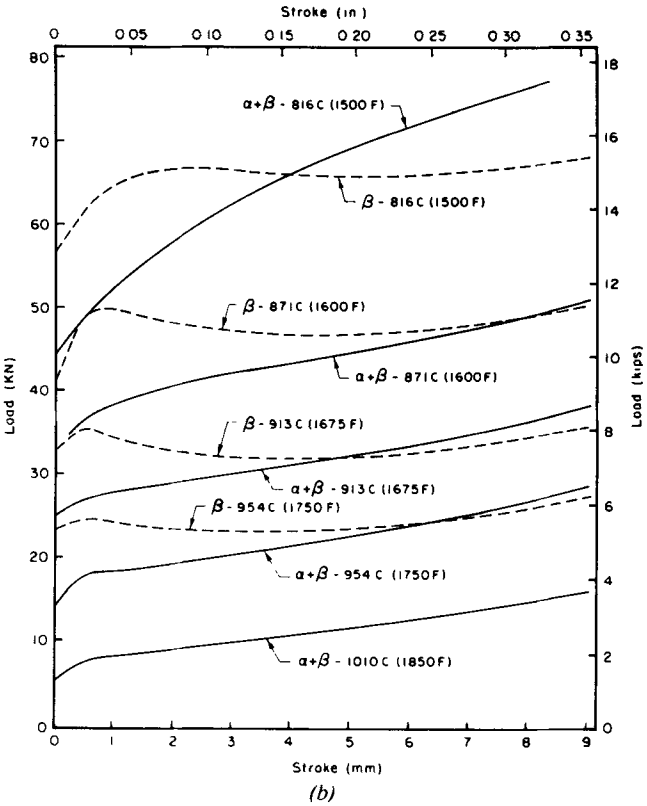

(b)

Fig. 2—Load-stroke curves for tests run on longitudinal specimens at (*a*) $\dot{\epsilon} = 0.1\ s^{-1}$ and (*b*) $\dot{\epsilon} = 1.0\ s^{-1}$.

True Stress-True Strain Curves. The difference in load-stroke curves for the two microstructures carries over to the true stress-true strain curves. (Sample curves for 0.1 and 1.0 s^{-1} are shown in Fig. 3.) The β microstructure stress-strain curves generally show much larger degrees of flow softening than the $\alpha + \beta$ stress-strain curves particularly at the lower test temperatures. In comparison with literature results for this and similar titanium alloys,[21,22,28,31] the $\alpha + \beta$ curves were concluded to be reliable. The small levels of flow softening observed for this microstructure are largely a result of the sharp dependence of flow stress on temperature and adiabatic heating during deformation. Further discussion and demonstration of this effect will follow. Suffice it to say for the present that without adiabatic heating, the stress-strain curves for this structure would show a short work-hardening stage followed by a flow stress plateau.* Metallographically, sections of deformed sam-

*Stress-strain data from 0.001 s^{-1} tests on the $\alpha + \beta$ microstructure (in which there was no adiabatic heating) showed a very small amount of flow softening. The softening in this case was attributed to α grain growth during the long testing times.

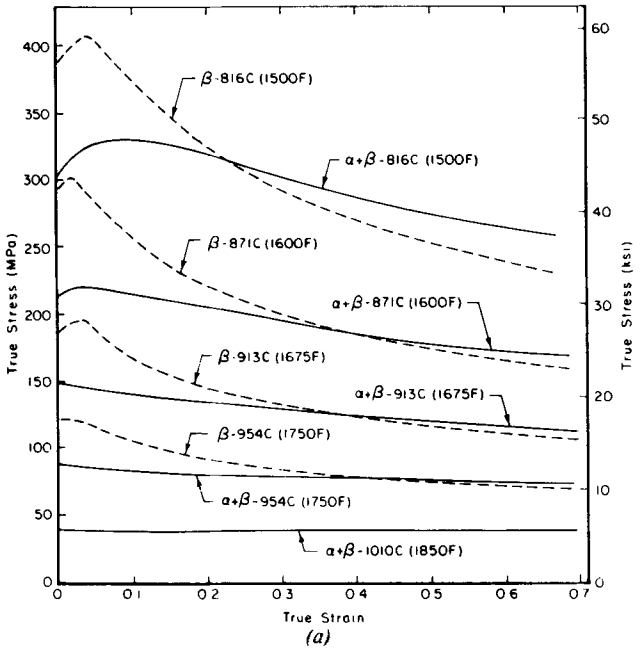

(a)

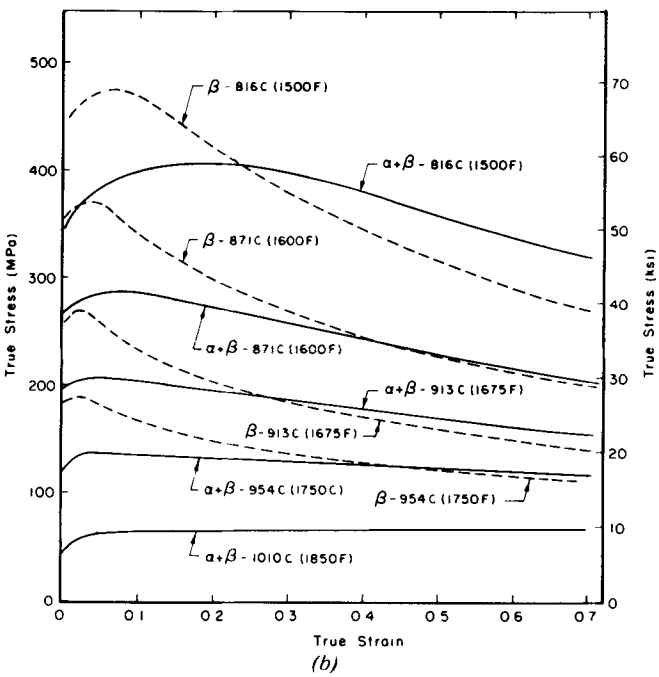

(b)

Fig. 3—True stress-true strain curves for tests run on longitudinal specimens at (*a*) $\dot{\epsilon} = 0.1\ s^{-1}$ and (*b*) $\dot{\epsilon} = 1.0\ s^{-1}$.

ples of the $\alpha + \beta$ microstructure showed α grains (in a transformed β matrix) elongated perpendicular to the compression axis. However, the degree of elongation was not as great as would be expected considering the imposed strain level. These observations, in conjunction with the stress-strain curves, lead to the conclusion that the deformation mechanism for the $\alpha + \beta$ microstructure consists of dynamic recovery[2] coupled with a certain amount of grain boundary sliding or migration.

The large levels of flow softening for the β microstructure cannot be attributed solely to adiabatic heating, as is the case for the $\alpha + \beta$ microstructure. Nor can the softening be ascribed to dynamic recrystallization, for gross recrystallization of the β microstructure to the (equilibrium) $\alpha + \beta$ microstructure was not observed in metallographic specimens. It was found though that a process involving localized deformation and changes in the morphology of the Widmanstatten platelet structure had occurred in β specimens (Fig. 4). Concomitant with this, electron microscopy studies have suggested that high, nonequilibrium levels of dislocations are present in Widmanstatten structures such as this and are reduced to the equilibrium level (for the given strain rate and temperature) by the deformation.[33] Hence, the β stress-strain curves approach and eventually join the $\alpha + \beta$ curves as the strain increases (Fig. 3).

Flow Stress-Temperature Plots. Modeling of deformation processes often requires knowledge of the flow stress as a function of strain, strain rate, and temperature. For this reason, the true stress-true strain data at a given rate were cross-plotted in terms of stress *vs* temperature at given levels of strain (data for 0.1 s^{-1}, for example, are shown in Fig. 5). Because of adiabatic heating, however, flow stress values at high strain levels for a test at a given nominal test temperature are actually representative of the deformation resistance at somewhat higher temperatures. The deformation was assumed to be adiabatic for strain rates of 0.1, 1.0, and 10.0 s^{-1}, and the temperature rises were calculated assuming 95 pct of the deformation work (area under the stress strain curve) is converted into heat:[28]

$$\Delta T = \frac{0.95 \int \sigma d\epsilon}{\rho c J}.$$

In this expression, ρ is the density and c is the specific heat of Ti-6242 at test temperatures and J is the mechanical equivalent of heat.[34]

Typical stress-temperature data corrected for adiabatic heating are shown in Fig. 6. It is seen that data for the $\alpha + \beta$ microstructure now fall on the same trend line except for low temperature-high strain rate com-

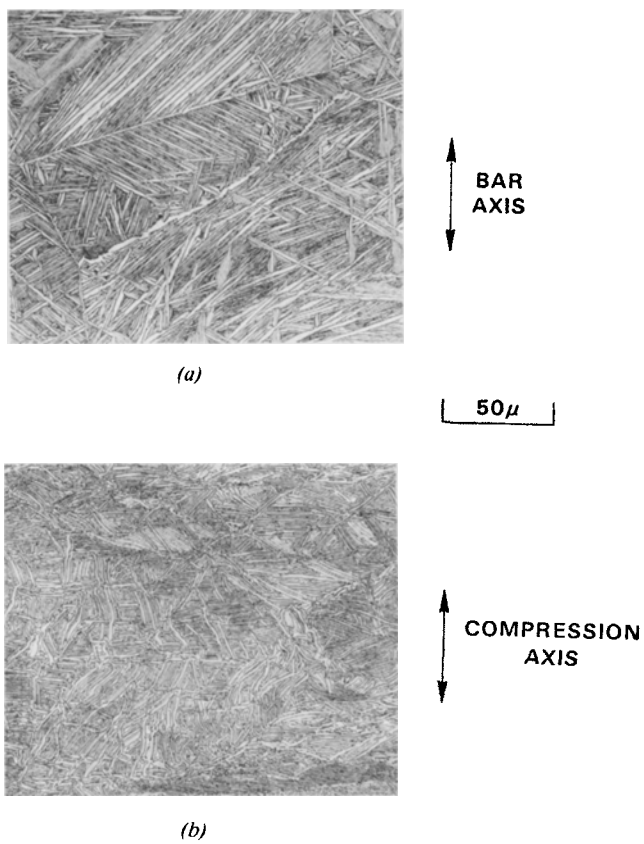

(a)

(b)

Fig. 4—Morphology of the β microstructure (*a*) as-β annealed and (*b*) after 50 pct reduction in height at 913 °C (1675 °F), $\dot{\epsilon} = 1.0\ s^{-1}$.

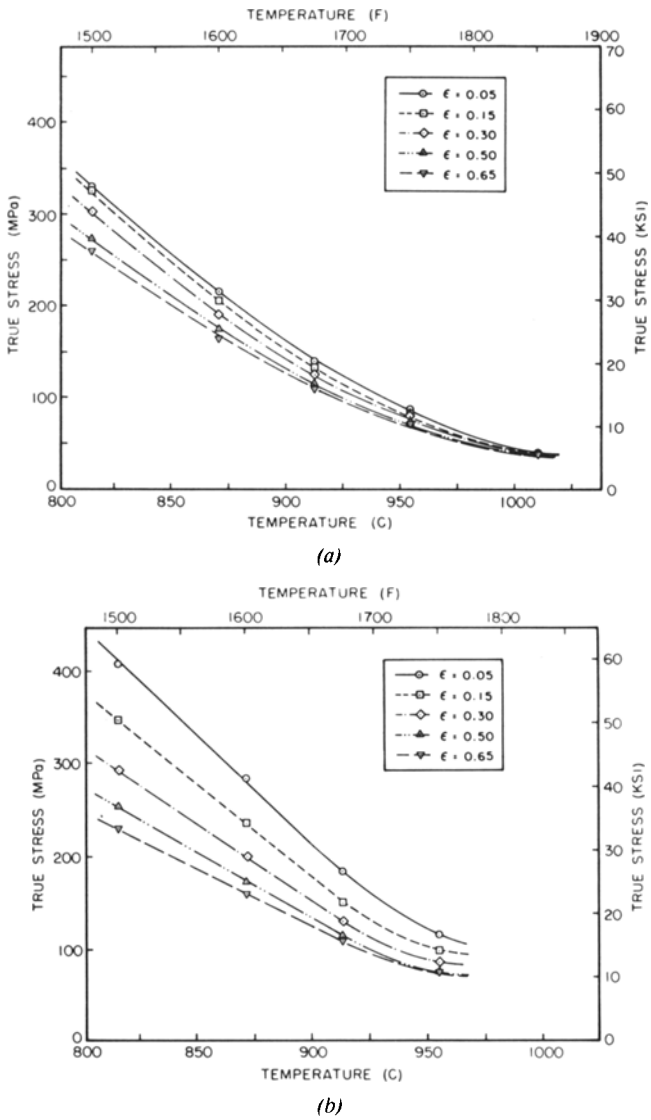

(a)

(b)

Fig. 5—Flow stress as a function of temperature at different strain levels: (*a*) $\alpha + \beta$ microstructure, $\dot{\epsilon} = 0.1\ s^{-1}$, and (*b*) β microstructure, $\dot{\epsilon} = 0.1\ s^{-1}$. All data from longitudinal direction.

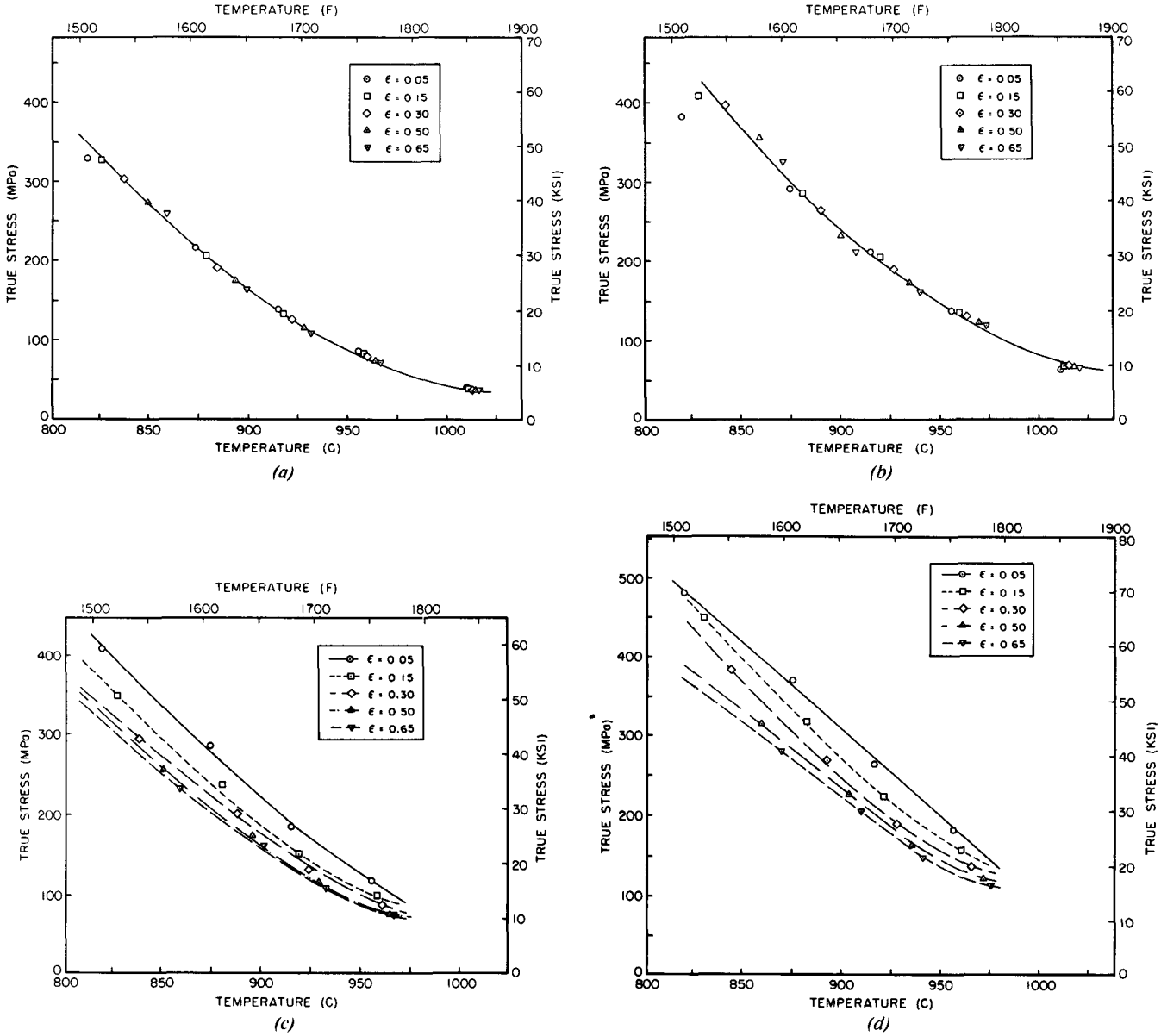

Fig. 6—Flow stress as a function of temperature after correction for adiabatic heating: (*a*) $\alpha + \beta$ microstructure, $\epsilon = 0.1\ s^{-1}$, (*b*) $\alpha + \beta$ microstructure, $\dot{\epsilon} = 1.0\ s^{-1}$, (*c*) β microstructure, $\dot{\epsilon} = 0.1\ s^{-1}$, and (*d*) β microstructure, $\dot{\epsilon} = 1.0\ s^{-1}$. All data from longitudinal direction.

binations. Therefore, it may be concluded that a truly isothermal high strain rate hot compression test for the $\alpha + \beta$ microstructure would yield a steady state flow stress dependent only on temperature and strain rate, but not strain, except at low temperatures and high strain rates where there is still a non-negligible amount of initial work-hardening in the flow curves. If the rule-of-mixtures has any effect on the hot deformation of two-phase structures, this result may seem surprising from a structural viewpoint since the percentage of the two phases varies with temperature. The flow stress (at a given strain rate) for the equilibrium structure preheated and tested at some particular temperature T^* may be expected to differ from that for a specimen of a structure which has been preheated at some lower temperature but which experiences deformation at T^* due to adiabatic heating. One plausible explanation for why this is not the case is that the grain boundary sliding, rather than matrix slip, may be the predominant deformation mechanism, and the α grain size does not vary considerably over the temperature intervals involved.

The temperature-corrected data for the β microstructure are also shown in Fig. 6. These plots confirm the conclusion that the majority of the flow softening for the β microstructure is not due to adiabatic heating. However, comparison of the $\alpha + \beta$ and β stress-temperature plots clearly illustrates how the β microstructure flow stresses converge to the $\alpha + \beta$ flow stresses at large strains.

Strain-Rate-Sensitivities. Log-log plots of flow stress *vs* strain rate were obtained from the temperature-corrected data for the $\alpha + \beta$ microstructure (*e.g.*, Figs. 6(*a*) and (*b*)) and from the temperature-corrected data for the β microstructure at $\epsilon = 0.30$ (*e.g.*, Figs. 6(*c*) and (*d*)). From these plots, application of Eq. [1]

enabled the determination of m, the strain rate sensitivity parameter (Fig. 7). The values so determined are similar to others reported in the literature for this alloy.[31,32] Although the strain rate sensitivities for the $\alpha + \beta$ microstructure tend to be higher than those for the β microstructure, their variation with temperature and strain rate is similar. For both microstructures, the m's increase with increasing temperature (up to the transus temperature at least) and decrease with increasing strain rate.

The large temperature dependence of the flow stress and large strain rate sensitivity of the flow stress for Ti-6242 are interrelated, and they may be correlated using the concepts of metal physics. If one assumes, as is the usual case in hot deformation, that the flow is controlled by a thermally activated process,[1] the flow stress may be considered to be a function of the Zener-Hollomon parameter, Z:[35]

$$\sigma = \sigma[\dot{\epsilon} \exp (Q/RT)] = \sigma[Z]. \qquad [2]$$

Q is the activation energy and R is the ideal gas constant. Taking the derivatives of Eq. [2] with respect to temperature and strain rate, one obtains:

$$\left.\frac{\partial \sigma}{\partial T}\right|_{\epsilon,\dot{\epsilon}} = \left[\frac{d\sigma}{dZ}\right]\left[\left.\frac{\partial Z}{\partial T}\right|_{\epsilon,\dot{\epsilon}}\right] = \left[\frac{d\sigma}{dZ}\right]\left[-\frac{Q\dot{\epsilon}}{RT^2}\exp (Q/RT)\right],$$

and

$$\left.\frac{\partial \ln \sigma}{\partial \ln \dot{\epsilon}}\right|_{T,\epsilon} = \frac{\dot{\epsilon}}{\sigma}\cdot\left.\frac{\partial \sigma}{\partial \dot{\epsilon}}\right|_{T,\epsilon} = \left[\frac{\dot{\epsilon}}{\sigma}\cdot\frac{d\sigma}{dZ}\right]\left[\left.\frac{\partial Z}{\partial \dot{\epsilon}}\right|_{T,\epsilon}\right] = \left[\frac{\dot{\epsilon}}{\sigma}\cdot\frac{d\sigma}{dZ}\right][\exp (Q/RT)].$$

Using the expression for Z (Eq. [2]), these equations become:

$$\left.\frac{\partial \sigma}{\partial T}\right|_{\epsilon,\dot{\epsilon}} = -\frac{QZ}{RT^2}\cdot\frac{d\sigma}{dZ}, \qquad [3]$$

and

$$m = \left.\frac{\partial \ln \sigma}{\partial \ln \dot{\epsilon}}\right|_{T,\epsilon} = \frac{Z}{\sigma}\cdot\frac{d\sigma}{dZ}. \qquad [4]$$

Dividing Eq. [4] by Eq. [3], and rearranging, we obtain the result:

$$m = -\frac{RT^2}{Q\sigma}\left[\left.\frac{\partial \sigma}{\partial T}\right|_{\epsilon,\dot{\epsilon}}\right]. \qquad [5]$$

Equation [5] was used to compare the m values predicted using the concepts of thermally activated processes to those from plots of log σ *vs* log $\dot{\epsilon}$ ("experimental measurements"). This was done at temperatures of 816, 871, 913, and 954 °C (1500, 1600, 1675, and 1750 °F). The values of Q employed were averages over the temperature and strain-rate range of interest and were determined from plots of log σ *vs* $1/T$. From Eq. [2], it is seen that at fixed σ, Q is given by:

$$\Delta \ln \dot{\epsilon} = -\frac{Q}{R}\Delta\left(\frac{1}{T}\right).$$

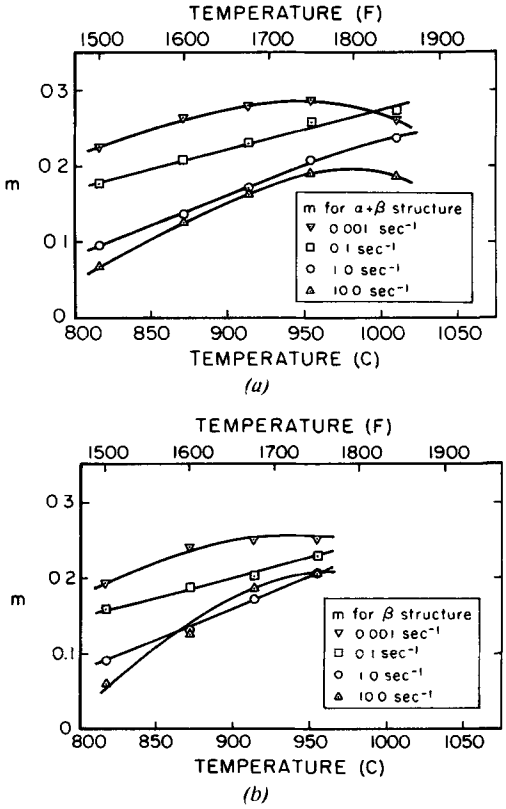

Fig. 7—Strain rate sensitivity parameters, m, for the (*a*) $\alpha + \beta$ microstructure and (*b*) β microstructure.

Activation energies, Q, of 149 and 146 kcal/mol were thus found for the $\alpha + \beta$ microstructure and the β microstructure, respectively. The values of $\partial\sigma/\partial T|_{\epsilon,\dot{\epsilon}}$ were obtained from the stress-temperature plots corrected for adiabatic heating (the unique trend lines for $\alpha + \beta$ data, and the $\epsilon = 0.30$ trend lines for β data).

Predictions from Eq. [5] are compared to "measurements" in Fig. 8. Error bars for the "measured" m values, if plotted in Fig. 8, would be ± 0.02. Agreement is good. This is particularly true in spite of the fact that

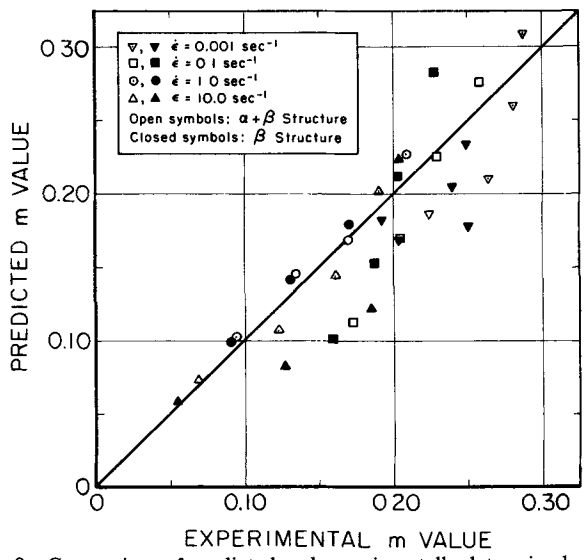

Fig. 8—Comparison of predicted and experimentally determined m values.

the structure is two-phase with phase proportions varying with temperature. In adddition, the good agreement supports the hypothesis that grain boundary sliding is an important deformation mechanism which may even be predominant over internal shear in the grains. If the latter were to predominate, one might expect to have to use some sort of rule of mixtures to obtain an expression analogous to Eq. [5] which is valid over the entire temperature range.

Nonisothermal Sidepressing

Results from nonisothermal sidepressing of cylinders of both microstructures underscore the important influence of a sharp temperature dependence of the flow stress in producing shear bands in hot forging. Metallographic sections showed that the development of these defects is similar in the two microstructures. The initial stage of shear band formation involves the development of chill zones in the hot workpiece adjacent to the cold dies (Figs. 9(*a*) and 10(*a*)). These zones offer a constraint to uniform flow in that their deformation is retarded by the locally high flow stress. As the deformation proceeds, these zones may deform slightly, but it appears that the material elements which undergo localized flow remain the same. The deformation can proceed either rather symmetrically about the compression axis intensifying the localized flow between the chill zones (Figs. 9(*b*) and 10(*b*)), or the chill zones can shift in opposite directions along the line of metal flow, which also tends to localize the flow very highly (Figs. 9(*c*) and 10(*c*)). The structures in the localized flow zones consist of very highly worked, unrecrystallized material (Fig. 11).

It is not surprising that the deformation behavior of the $\alpha + \beta$ and β microstrucrures is similar in nonisothermal sidepressing. In these forging situations, the formation of chill zones determines the occurrence and extent of localized flow. Thus, thermal properties, and the overall flow stress dependence on temperature and strain rate are the important material variables, and since they are similar for the two structures (*e.g.*, compare σ-T plots in Fig. 6), the present observations are credible. One must not forget, however, the importance of working speed, die temperature, and lubrication in the formation of these nonisothermal shear bands because these variables play a critical role in the heat transfer process which sets the stage for the formation of the chill zones. Proper selection of these variables (*e.g.*, increased working speed, increased die temperature) can eliminate these defects. Work is now underway to more firmly establish this deduction.

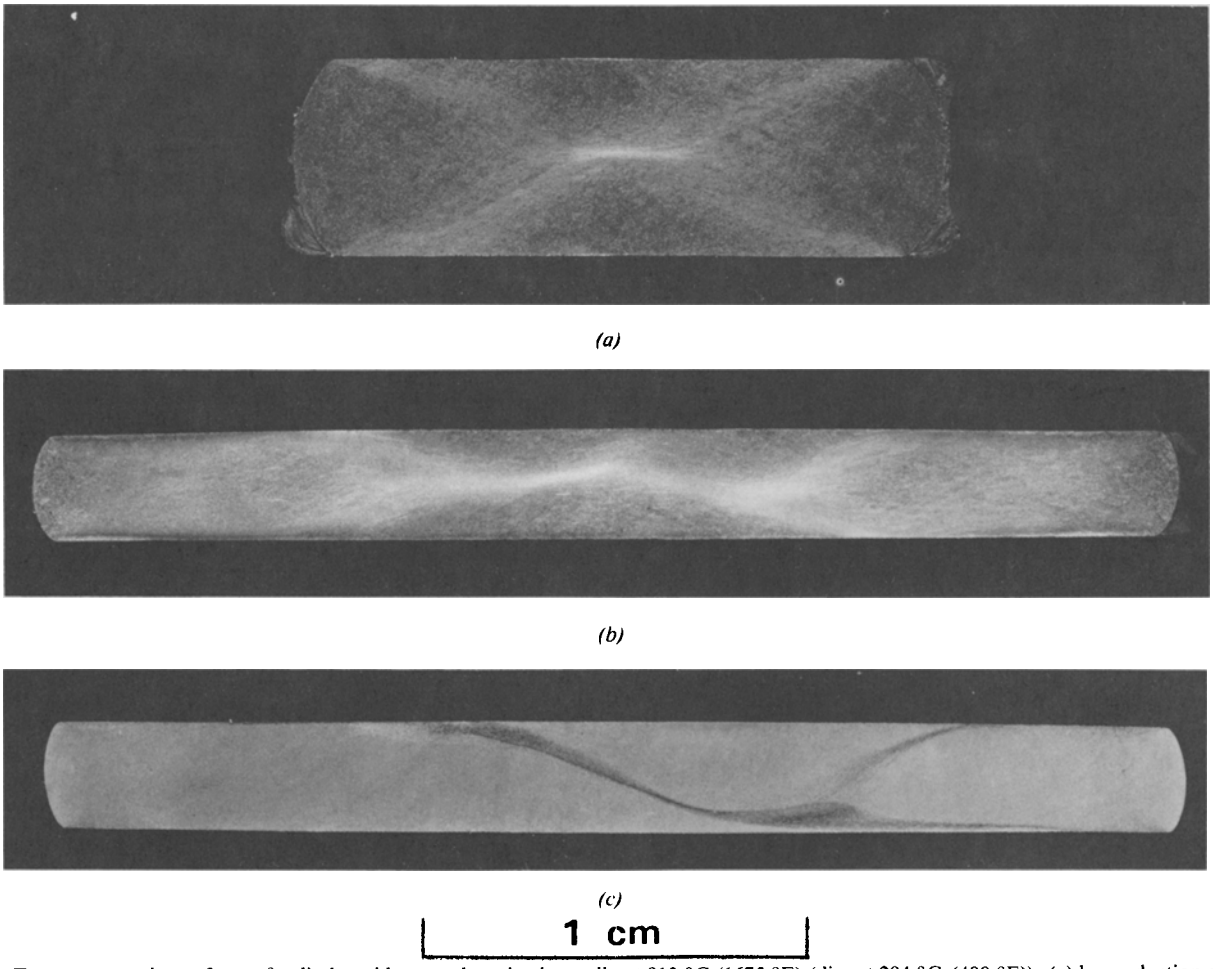

Fig. 9—Transverse sections of $\alpha + \beta$ cylinders sidepressed nonisothermally at 913 °C (1675 °F) (dies at 204 °C (400 °F)): (a) low reduction and (*b*), (*c*) large reduction. $\dot{\epsilon} \approx 30\ s^{-1}$.

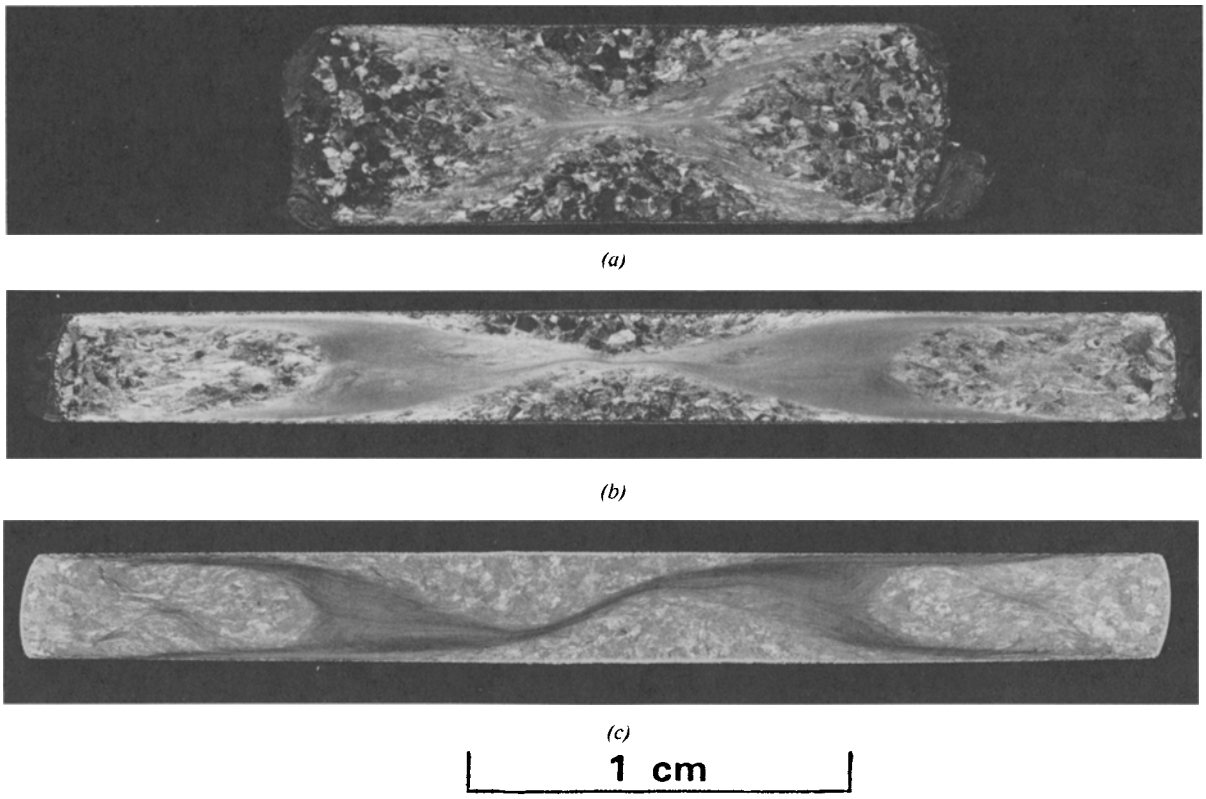

Fig. 10—Transverse sections of β cylinders sidepressed nonisothermally at 913 °C (1675 °F) (dies at 204 °C (400 °F)): (*a*) low reduction and (*b*), (*c*) large reduction. $\dot{\epsilon} = 30\ s^{-1}$.

Isothermal Sidepressing

Observations. Isothermally sidepressed cylinders of Ti-6242 also showed evidence of shear localization along directions reminiscent of the velocity discontinuities of skip-line field theory.[31] However, the occurrence of shear bands was different for the two microstructures. At the lower test temperature of 843 °C (1550 °F), the $\alpha + \beta$ microstructure developed weak shear bands (Fig. 12(*a*)). The degree of localization in this isothermal case (Fig. 13) does not appear as severe as that in the nonisothermal case (Fig. 11(*a*)), although the deformation levels are similar. At the higher test temperature of 913 °C (1675 °F), this microstructure deformed uniformly with no evidence of flow localization (Fig. 12(*b*)). In contrast, the β microstructure formed shear bands at both test temperatures (Fig. 14). In both cases, these shear deformations involved very large strains compared to the overall deformation outside the locaized flow regions (Fig. 15). In fact, the strain and temperature were high enough that the material in the shear bands formed at 913 °C (1675 °F) dynamically recrystallized to form the equilibrium equiaxed alpha microstructure.

Analysis. The mode of flow instability and flow localization in plane-strain sidepressing may be analyzed in a manner analogous to that employed by Jonas, *et al*,[30] and Dadras and Thomas[32] to predict the onset of unstable bulging in uniaxial compression. For unstable bulging in compression, the instability condition is

$$dF = \sigma dA + A d\sigma = 0.$$

A is the instantaneous cross-sectional area of the specimen. On the other hand, for localization along a direction of pure shear it follows that $d\sigma = 0$ is the necessary condition for instability since in this case $dA = 0$.[36]

If we consider the flow stress σ to be a function of strain ϵ, strain rate $\dot{\epsilon}$, and temperature T, the instability condition is:

$$d\sigma = 0 = \left(\frac{\partial \sigma}{\partial \epsilon}\bigg|_{\dot{\epsilon},T}\right) d\epsilon + \left(\frac{\partial \sigma}{\partial \dot{\epsilon}}\bigg|_{\epsilon,T}\right) d\dot{\epsilon} + \left(\frac{\partial \sigma}{\partial T}\bigg|_{\epsilon,\dot{\epsilon}}\right) dT. \quad [6]$$

Noting that

$$\gamma' \equiv \frac{1}{\sigma}\frac{d\sigma}{d\epsilon}\bigg|_{\epsilon} = \left\{\left(\frac{\partial \sigma}{\partial \epsilon}\bigg|_{\dot{\epsilon},T}\right) d\epsilon + \left(\frac{\partial \sigma}{\partial T}\bigg|_{\epsilon,\dot{\epsilon}}\right) dT\right\} / \sigma d\epsilon,$$

and

$$m = \frac{\partial \ln \sigma}{\partial \ln \dot{\epsilon}}\bigg|_{\epsilon,T} = \frac{\dot{\epsilon}}{\sigma}\left(\frac{\partial \sigma}{\partial \dot{\epsilon}}\bigg|_{\epsilon,T}\right),$$

Equation [6] becomes

$$0 = \gamma' \sigma d\epsilon + \frac{\sigma}{\dot{\epsilon}} m d\dot{\epsilon}. \quad [7]$$

Rearranging,

$$\frac{1}{\dot{\epsilon}}\frac{d\dot{\epsilon}}{d\epsilon} = -\frac{\gamma'}{m} = \alpha. \quad [8]$$

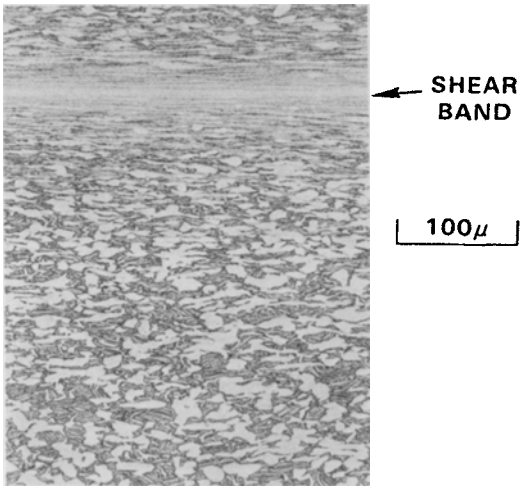

(a)

(b)

Fig. 11.—Micrographs showing shear bands in nonisothermally sidepressed specimens of (*a*) $\alpha + \beta$ microstructure and (*b*) β microstructure. Specimen $T = 913$ °C (1675 °F), die $T = 204$ °C (400 °F), $\dot{\epsilon} \approx 30\ s^{-1}$.

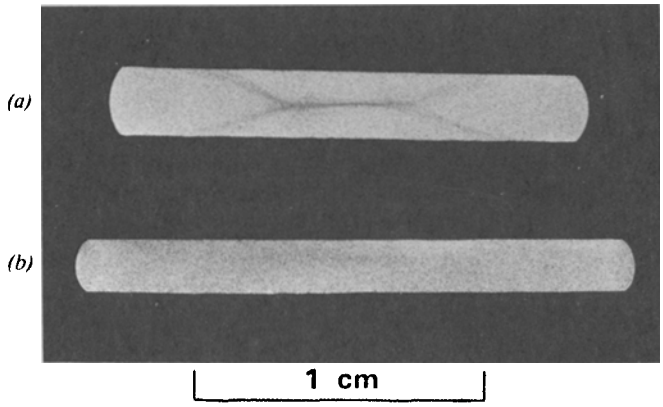

Fig. 12—Transverse sections of isothermally sidepressed cylinders of the $\alpha + \beta$ microstructure: (*a*) sidepressed at 843 °C (1550 °F) and (*b*) sidepressed at 913 °C (1675 °F). $\dot{\epsilon} \approx 10\ s^{-1}$.

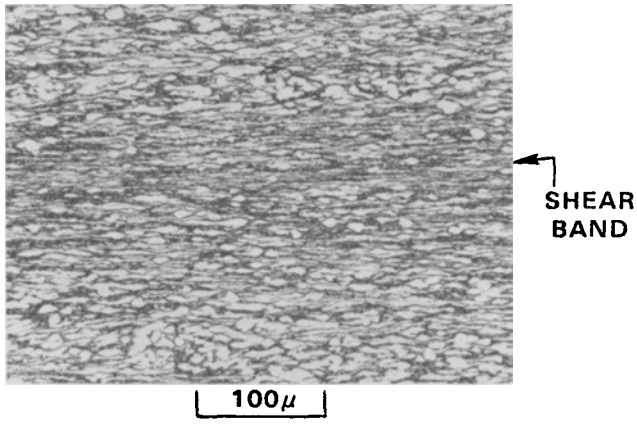

Fig. 13—Shear band in isothermally sidepressed specimen of $\alpha + \beta$ microstructure. Test $T = 843$ °C (1550 °F), $\dot{\epsilon} \approx 10\ s^{-1}$

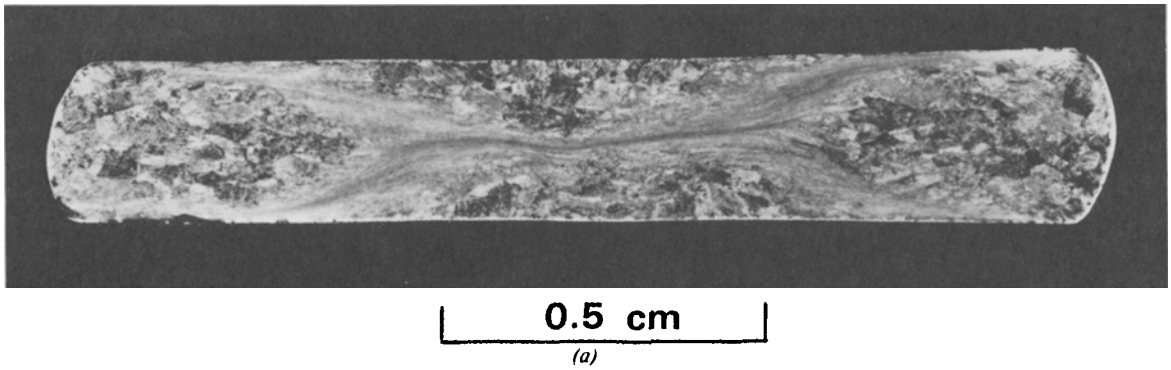

(a)

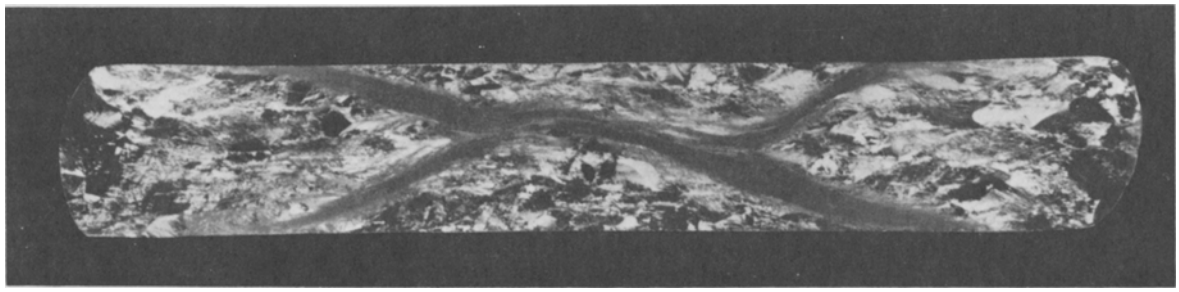

(b)

Fig. 14—Isothermally sidepressed cylinders of the β microstructures: (*a*) transverse section of cylinder deformed at 843 °C (1550 °F) and (*b*) transverse section of cylinder derformed at 913 °C (1675 °F). $\dot{\epsilon} \approx 10\ s^{-1}$.

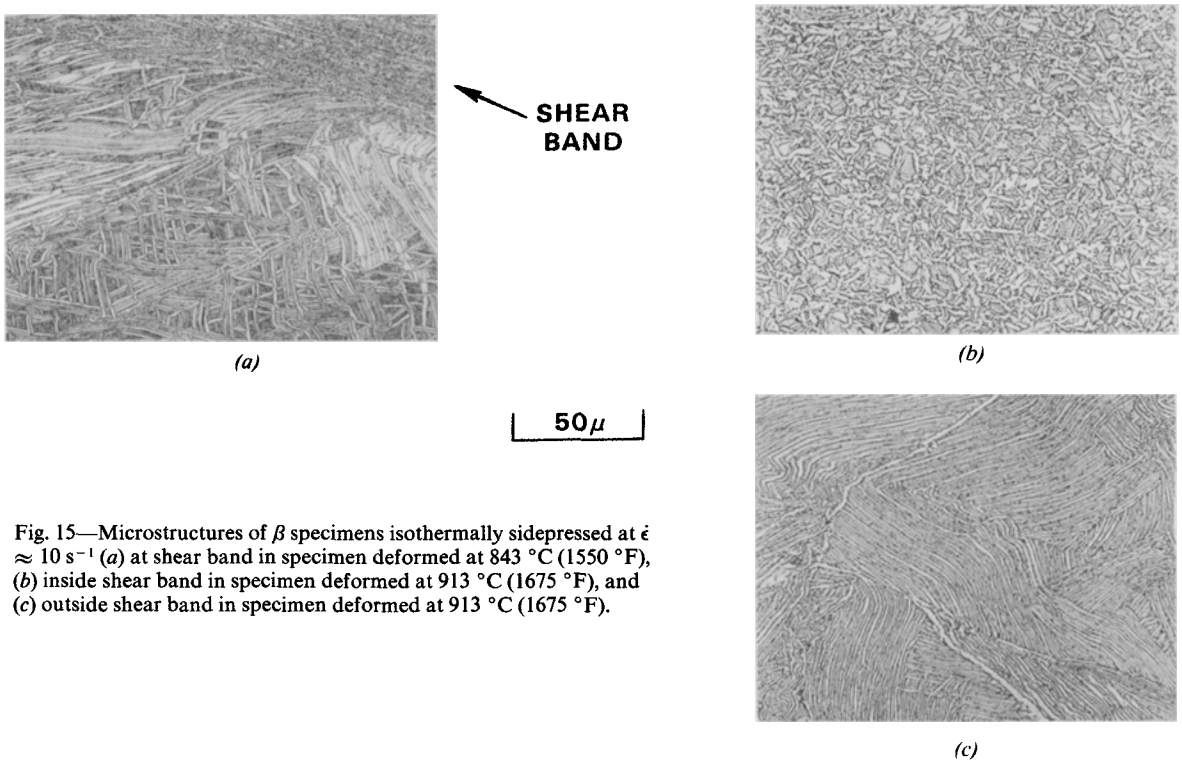

Fig. 15—Microstructures of β specimens isothermally sidepressed at $\dot{\epsilon} \approx 10\ s^{-1}$ (*a*) at shear band in specimen deformed at 843 °C (1550 °F), (*b*) inside shear band in specimen deformed at 913 °C (1675 °F), and (*c*) outside shear band in specimen deformed at 913 °C (1675 °F).

The quantity $(1/\dot{\epsilon})d\dot{\epsilon}/d\epsilon$, the fractional change of strain rate with strain, is the parameter most often used to gage the tendency of materials to undergo localized flow if the material is prone to instability. Jonas[30] suggests that materials with α parameters of 5 or greater are particularly susceptible to persistent flow localizations. With this criterion, observations of shear bands in Ti-6242 can be interpreted.

Application of Analysis. From Eq. [8], the α parameters for the deformation of the $\alpha + \beta$ and β microstructures were calculated (Tables I and II). The values of $\gamma' = (1/\sigma)(\partial\sigma/\partial\epsilon)|_{\dot{\epsilon}}$ were obtained directly from the longitudinal stress-strain curves *not* corrected for adiabatic heating (*e.g.*, Fig. 3) and m's were obtained as discussed before. (Strain localization parameters calculated using transverse direction stress-strain properties and m values are very similar to those given in Tables I and II.) As Table I shows, the $\alpha + \beta$ microstructure shows little tendency for flow localization along shear bands except at low temperatures and high strain rates. In no cases do the α parameters exceed 5 except for T's in the range 816 to 871 °C (1500 to

Table I. Flow Localization Parameter, α, for Ti-6242 of $\alpha + \beta$ Microstructure

Nominal Test Temperature (°C(F))	Strain Rate (s^{-1})	$\alpha(\epsilon = 0.10)$	$\alpha(\epsilon = 0.225)$	$\alpha(\epsilon = 0.40)$	$\alpha(\epsilon = 0.575)$
816(1500)	0.001	3.4	2.6	2.1	1.8
	0.100	0.4	3.0	2.9	2.0
	1.00	< 0	1.9	5.9	6.2
	10.0	< 0	1.3	5.1	9.7
871(1600)	0.001	2.4	2.2	1.6	1.1
	0.100	2.1	2.6	2.2	1.8
	1.00	1.6	4.0	4.8	4.4
	10.0	< 0	2.7	4.2	4.4
913(1675)	0.0001	3.1	2.7	1.9	0.9
	0.100	2.1	1.7	1.9	1.2
	1.00	2.0	3.1	2.9	2.8
	10.0	0.3	2.4	2.5	4.0
954(1750)	0.001	0.9	1.3	1.0	1.4
	0.100	1.6	0.9	1.1	1.0
	1.00	1.0	1.2	1.4	1.1
	10.0	< 0	0.7	2.1	0.0
1010(1850)	0.001	2.1	1.4	0.9	0.0
	0.100	0.6	0.0	0.3	0.4
	1.00	< 0	< 0	0.2	0.6
	10.0	< 0	< 0	0.9	1.4

Table II. Flow Localization Parameter, α, for Ti-6242 of β Microstructure

Nominal Test Temperature (°C(F))	Strain Rate (s^{-1})	$\alpha(\epsilon = 0.10)$	$\alpha(\epsilon = 0.225)$	$\alpha(\epsilon = 0.40)$	$\alpha(\epsilon = 0.575)$
816(1500)	0.001	6.8	4.6	4.2	3.8
	0.100	9.9	7.1	4.6	4.0
	1.00	7.8	12.0	10.6	9.0
	10.0	< 0	14.2	20.2	16.2
871(1600)	0.001	5.4	4.7	3.8	2.6
	0.100	10.2	5.8	3.9	2.6
	1.00	11.9	8.5	6.5	5.1
	10.0	4.9	8.0	1.5	6.1
913(1675)	0.001	6.2	4.1	3.3	2.3
	0.100	10.1	5.1	3.2	1.6
	1.00	10.1	6.3	4.4	3.7
	10.0	4.5	4.9	4.7	4.3
954(1750)	0.001	7.2	4.5	3.6	2.0
	0.100	7.7	4.2	2.7	2.0
	1.00	7.4	4.6	2.9	2.3
	10.0	4.7	4.6	3.1	2.5

1600 °F) at strain rates $\dot{\epsilon} \gtrsim 1\ s^{-1}$. In addition, the localization parameter does not reach a "critical" value until relatively large strains ($\epsilon \gtrsim 0.40$). In view of these predictions, it is not surprising that shear bands were found at 843 °C (1550 °F), $\dot{\epsilon} \approx 10\ s^{-1}$ and not at 913 °C (1675 °F), $\dot{\epsilon} \approx 10\ s^{-1}$.

In contrast to the predictions for the $\alpha + \beta$ microstructure, the flow localization parameters for the β microstructure (Table II) are very large. They exceed 5 at some strain level for all temperature-strain-rate combinations, except for 913 °C (1675 °F) – $10\ s^{-1}$ and 954 °C (1750 °F) – $10\ s^{-1}$, for which its maximum values are 4.9 and 4.7, respectively, which are still very large. Furthermore, the parameters in all cases assume large values at low strains ($\epsilon = 0.10$ or 0.225), and, therefore, initiation of shear bands can be expected to occur early in the deformation. These predictions are supported by the shear band observations for the β sidepressings at 843 °C (1550 °F), $\dot{\epsilon} \approx 10\ s^{-1}$ and at 913 °C (1675 °F), $\dot{\epsilon} \approx 10\ s^{-1}$. The good definition of the shear bands in these cases supports the prediction of early initiation as well. Work is now underway to further document the applicability of Eq. [8] for the prediction of shear bands in the $\alpha + \beta$ and β structures at other temperatures, strain rates, and deformation levels.

SUMMARY AND CONCLUSIONS

The deformation and unstable flow during hot forging of Ti-6242 were studied using isothermal hot compression testing and nonisothermal and isothermal lateral sidepressing. The following conclusions were drawn:

1) During simple compression, the flow behavior is determined largely by the starting microstructure. The equiaxed, $\alpha + \beta$ microstructure exhibited monotonically increasing load-stroke curves and deformed stably at all temperatures and strain rates. In contrast, the Widmanstatten, or transformed β, microstructure showed decreasing load-stroke curves and somewhat nonuniform deformation.

2) In terms of stress-strain behavior, the $\alpha + \beta$ microstructure had a nearly constant flow stress. Small decreases in flow stress during straining could be ascribed to adiabatic heating and a sharp dependence of flow stress on temperature. On the other hand, the β microstructure had stress-strain curves which showed large degrees of flow softening, or decreases of flow stress with straining. Only a small portion of this behavior could be attributed to adiabatic heating. The remainder arises from changes in the original, nonequilibrium microstructure, including modification of the Widmanstatten morphology and dislocation substructure.

3) The large dependence of flow stress on temperature for both microstructures is interrelated with the large strain rate sensitivity of the flow stress. An expression relating the two was derived, and its applicability to the data for Ti-6242 was established. In addition, the analysis demonstrated that the deformation of Ti-6242 at hot working temperatures and strain rates is largely a thermally activated process with minimal influences from viscous drag.

4) The large dependence of flow stress on temperature plays an important role in the occurrence of shear bands in nonisothermally forged Ti-6242. It was shown that this characteristic enhances the development of chill zones (zones of little or no deformation in contact with the dies) which constrain deformation and localize flow. Both Ti-6242 microstructures exhibited shear bands from nonisothermal sidepressing, underlining the importance of process variables (*e.g.*, die temperature and working speed) as well as the general dependence of flow stress on temperature and strain rate in producing the defects.

5) Shear bands were also observed in isothermal sidepressing . In this case, localization was found to depend principally on the rate of flow softening and the strain rate sensitivity of the flow stress, which vary with microstructure, deformation temperature, and deformation rate. It was postulated that when the ratio of the nondimensional flow softening rate to the strain rate sensitivity parameter was equal to or greater than 5,

shear bands are likely, at least in plane strain deformation. Observations of shear bands at 843 °C (1550 °F), but not at 913 °C (1675 °F), in specimens of the $\alpha + \beta$ structure supported the theory developed for their prediction. Observations of shear bands at both of these temperatures in specimens of the β microstructure also were used to validate the theory.

ACKNOWLEDGMENTS

This research was graciously supported by the Air Force Office of Scientific Research, Air Force Systems Command, USAF, under Grant No. AFOSR-79-004 (A. Rosenstein, Program Manager). Many enlightening technical discussions with Dr. A. Hoffmanner and Dr. T. Altan helped in the formulation of much of the work reported here. In addition, the assistance of Messrs. N. Frey, W. W. Sunderland, and C. R. Thompson in performance of the experimental work is greatly appreciated. Dr. C. C. Chen of Wyman-Gordon Co. kindly supplied the materials used in the investigation.

REFERENCES

1. W. J. McG. Tegart: *Ductility*, p. 133, ASM, Metals Park, OH, 1968.
2. J. J. Jonas and H. J. McQueen: *Treatise on Materials Science and Technology, Vol. 6: Plastic Deformation of Metals*, R. J. Arsenault, ed., p. 394, Academic Press, New York, 1975.
3. J. J. Jonas: *Proc. Fourth Inter. Conf. on the Strength of Metals and Alloys*, Nancy, France, Aug. 30–Sept. 3, 1976, p. 976.
4. J. J. Jonas and M. J. Luton: *Advances in Deformation Processing*, p. 215, Plenum Press, New York, 1978.
5. C. M. Young and O. D. Sherby: *Metal Forming—Interrelation between Theory and Practice*, A. L. Hoffmanner, ed., p. 429, Plenum Press, New York, 1971.
6. K. A. Reynolds: *Deformation under Hot Working Conditions*, C. M. Sellars and W. J. McG. Tegart, eds., p. 107, Iron and Steel Institute, London, 1968.
7. B. J. Sunter and N. M. Burman: *J. Aust. Inst. Met.*, 1972, vol. 17, p. 91.
8. R. C. Koeller and R. Raj: *Acta Metall.*, 1978, vol. 26, p. 1551.
9. H. C. Rogers: *Ann. Rev. Mater. Sci.*, 1979, vol. 9, p. 283.
10. J. Pomey: *Annals of the C.I.R.P.*, 1966, vol. 13, p. 93.
11. S. Kobayashi, C. H. Lee, Y. Saida, and S. C. Jain: Technical Report AFML-TR-70-90, University of California, Berkeley, CA, July, 1970.
12. K. Brown: *J. Inst. Met.*, 1972, vol. 100, p. 341.
13. M. N. Janardhana and S. K. Biswas: *Int. J. Mech. Sci.*, 1979, vol. 21, p. 699.
14. W. Johnson, G. L. Baraya, and R. A. C. Slater: *Int. J. Mech. Sci.*, 1964, vol. 6, p. 409.
15. R. H. Ernst and J. W. Spretnak: *Trans. Iron Steel Inst. Jpn.*, 1969, vol. 9, p. 361.
16. D. Hauser: Ph.D. Thesis, Ohio State University, Department of Metallurgical Engineering, Columbus, OH, 1973.
17. V. Osina: *Met. Treat.*, May, 1966, vol. 33, p. 193.
18. A. L. Hoffmanner: Unpublished research, TRW, Inc., Cleveland, OH, 1970.
19. G. L. Wulf: *Int. J. Mech. Sci.*, 1979, vol. 21, p. 713.
20. F. N. Lake and D. J. Moracz: Technical Report AFML-TR-71-112, TRW, Inc., Cleveland, OH, May, 1971.
21. A. L. Hoffmanner: Technical Report AFML-TR-69-174, TRW, Inc., Cleveland, OH, June, 1969.
22. A. J. Griest, A. M. Sabroff, and P. D. Frost: *Trans. Am. Soc. Met.*, 1959, vol. 51, p. 935.
23. A. U. Sulijoadikusumo and O. W. Dillon, Jr.: *Metallurgical Effects at High Strain Rates*, R. W. Rohde, ed., p. 501, Plenum Press, New York, 1973.
24. C. C. Chen and J. E. Coyne: *Metall. Trans. A*, 1976, vol. 7A, p. 1931.
25. C. C. Chen: Report RD-77-110, Wyman-Gordon Co., North Grafton, MA, October, 1977.
26. H. A. Kuhn: Unpublished research, University of Pittsburgh, Pittsburgh, PA, 1979.
27. T. Altan: Report MCIC-HB-03, p. 1, Metals and Ceramics Information Center, Columbus, OH, October, 1973.
28. J. R. Douglas and T. Altan: Report No. AMMRC CTR 72-25, Battelle's Columbus Laboratories, Columbus, OH, November, 1972.
29. W. A. Backofen: *Deformation Processing*, chapt. 10, Addison-Wesley Publishing Company, Reading, MA, 1972.
30. J. J. Jonas, R. A. Holt, and C. E. Coleman: *Acta Metall.*, 1976, vol. 24, p. 911.
31. S. L. Semiatin, G. D. Lahoti, and T. Altan: *Process Modeling: Fundamentals and Applications to Metals*, T. Altan, H. Burte, H. Gegel, and A. Male, eds., p. 387, ASM, Metals Park, OH, 1980.
32. P. Dadras and J. Thomas: *Res Mechanica Letters*, 1981, vol. 1, p. 97.
33. D. J. Abson and J. J. Jonas: *Met. Technol.*, 1977, vol. 4, p. 462.
34. H. A. Russell: TMCA Case Study M-109, June, 1967.
35. C. Zener and J. H. Hollomon: *J. Appl. Phys.*, 1944, vol. 15, p. 22.
36. A. K. Chakrabarti and J. W. Spretnak: *Metall. Trans. A*, 1975, vol. 6A, p. 733.